AIMS Energy, 11(2): 271–292.
DOI: 10.3934/energy.2023015
Received: 21 September 2022
Revised: 08 March 2023
Accepted: 14 March 2023
Published: 17 March 2023

http://www.aimspress.com/journal/energy

Research article

Contribution of a power multivector to distorting load identification

Anthoula Menti, Dimitrios Barkas, Pavlos Pachos, and Constantinos S. Psomopoulos*

Department of Electrical and Electronics Engineering, University of West Attica, Egaleo 12241, Athens, Greece

* **Correspondence:** Email: cpsomop@uniwa.gr; Tel: +302105381182.

Abstract: The identification of harmonic generating loads and the assignation of responsibility for harmonic pollution is an important first step for harmonic control in modern power systems. In this paper, a previously introduced power multivector is examined as a possible tool for the identification of such loads. This representation of power is based on the mathematical framework of Geometric Algebra (GA). Components of the power multivector derived at the point of connection of a load are grouped into a single quantity, which is a bivector in GA and is characterized by a magnitude, direction and sense. The magnitude of this bivector can serve as an indicator of the distortion at the terminals of the load. Furthermore, in contrast to indices based solely on magnitude, such as components derived from any apparent power equation, the proposed bivectorial representation can differentiate between loads that enhance distortion and those with a mitigating effect. Its conservative nature permits an association between the distortion at specific load terminals and the common point of connection. When several loads connected along a distribution line are considered, then an evaluation of the impact of each one of these loads on the distortion at a specific point is possible. Simulation results confirm that information included in the proposed bivector can provide helpful guidance when quantities derived from apparent power equations deliver ambiguous results.

Keywords: power theory; power system harmonics; distorting load identification

Nomenclature: $u(t)$: Voltage time function [V]; $i(t)$: Current time function [A]; U: Voltage rms value [V]; I: Current rms value [A]; U_i: Rms value of i-th voltage harmonic [V]; I_i: Rms value of i-th current harmonic [A]; α_i: Phase angle of i-th voltage harmonic; β_i: Phase angle of i-th current harmonic; φ_i: Phase difference of i-th harmonic voltage and current; **u**: Voltage vector [V]; **i**:

Current vector [A]; S: Apparent power [VA]; P: Active power [W]; Q: Reactive power [Var]; D_B: Budeanu's distortion power [VA]; Q_B: Budeanu's reactive power [VA]; Q_F: Fryze's reactive power [VA]; S_Q: Sharon's quadrature reactive power [VA]; S_I: Fundamental apparent power [VA]; D_I: Current distortion power [VA]; D_V: Voltage distortion power [VA]; S_H: Harmonic apparent power [VA]; $\mathbf{S}$: Power multivector [VA]; P_{ii}: Active power of i-th harmonic [W]; Q_{ii}: Reactive power of i-th harmonic [Var]; $\mathbf{Q}$: Reactive power bivector [Var]; $\mathbf{Q}_{ii}$: Reactive power bivector of i-th harmonic [Var]; $\mathbf{P}_M$: Nonactive power bivector associated with in-phase current components [VA]; $\mathbf{Q}_M$: Nonactive power bivector associated with quadrature current components [VA]; $\mathbf{P}_{Mij}$: Nonactive power bivector associated with i-th harmonic voltage and j-th harmonic current component in phase with its respective voltage harmonic [VA]; P_{Mij}: Magnitude of $\mathbf{P}_{Mij}$ [VA]; $\mathbf{Q}_{Mij}$: Nonactive power bivector associated with i-th harmonic voltage and j-th harmonic current component in quadrature with its respective voltage harmonic [VA]; Q_{Mij}: Magnitude of $\mathbf{Q}_{Mij}$ [VA]; $\mathbf{B}_M$: Generalized Mutual Coupling (GMC) bivector [VA]; $\mathbf{B}_{Mh}$: Component of $\mathbf{B}_M$ associated with harmonics up to the 50th order [VA]; $\mathbf{B}_{Msh}$: Component of $\mathbf{B}_M$ associated with supraharmonics [VA]; $u_x(t)$: Voltage of load x time function [V]; $i_x(t)$: Current of load x time function [A]; $\alpha_{x,i}$: Phase angle of i-th voltage harmonic of load x; $\beta_{x,i}$: Phase angle of i-th current harmonic of load x; $\varphi_{x,i}$: Phase difference of i-th harmonic voltage and current of load x; $\theta_{x,i}$: Phase difference between the voltage at a common point of connection and the voltage of load x; $U_{x,i}$: Rms value of i-th voltage harmonic of load x [V]; $I_{x,i}$: Rms value of i-th current harmonic of load x [A]; $\mathbf{u}_x$: Voltage vector of load x [V]; $\mathbf{i}_x$: Current vector of load x [A]; $\mathbf{S}_x$: Power multivector of load x [VA]; $P_{x,ii}$: Active power of i-th harmonic of load x [W]; $Q_{x,ii}$: Reactive power of i-th harmonic of load x [Var]; $P_{Mx,ij}$: Magnitude of nonactive power bivector of load x associated with i-th harmonic voltage and j-th harmonic current component in phase with its respective voltage harmonic [W]; $Q_{Mx,ij}$: Magnitude of nonactive power bivector of load x associated with i-th harmonic voltage and j-th harmonic current component in quadrature with its respective voltage harmonic [Var]; $\mathbf{B}_{Mx}$: GMC bivector of load x [VA]; $\mathbf{B}_{Mxp}$: Component of $\mathbf{B}_{Mx}$ parallel to the GMC bivector $\mathbf{B}_M$ at a common point of connection [VA]; $\mathbf{B}_{Mxr}$: Component of $\mathbf{B}_{Mx}$ orthogonal to the GMC bivector $\mathbf{B}_M$ at a common point of connection [VA]; b_{Mx}, b_{Mhx}, b_{Mshx}: Coefficients of contribution of load x to $\mathbf{B}_M$, $\mathbf{B}_{Mh}$ and $\mathbf{B}_{Msh}$ respectively

1. Introduction

1.1. Motivation and incitement

Power quality is one of the most prominent topics in modern power engineering literature. Among the numerous problems classified as power quality disturbances, power system harmonics are a serious concern for utilities and consumers alike. The growing awareness regarding the environmental impact of fossil fuel consumption as well as their impending depletion has given rise to a quest for more energy-efficient electronic equipment in industrial, commercial and residential installations. Nonlinear loads such as LED lamps, industrial converters, electronic power supplies and battery chargers are becoming increasingly common. The integration of renewable energy systems into utility grids is also rapidly growing, with photovoltaic (PV) systems emerging as major contributors to energy generation. In addition to large scale photovoltaic power plants, small scale PV installations on rooftops connected to the low voltage utility grid are practically commonplace. Furthermore, new kinds of equipment incorporating power electronic converters, such as electric

vehicle (EV) battery chargers are expected to proliferate in the future. All these devices tend to inject harmonics into the grid at the point of their connection. The harmonic currents generated by these devices cause a corresponding voltage drop on the distribution line impedance resulting in a distorted voltage supply for all loads.

Waveform distortion in power systems can result in increased losses and heating in transformers and motors. It can also cause interference with communication circuits and malfunction of electronic equipment. The identification of harmonic generating customers is an important first step in controlling harmonic levels in the grid. By identifying harmonic emitting loads, appropriate mitigation solutions can be considered [1–3].

1.2. Literature review

Various approaches for distorting load identification have been presented in the literature [4–11]. They are usually classified into multipoint and single-point methods. The former involve multiple measurement points and synchronous distributed measurements. Their superior accuracy is offset by the complexity of the required equipment and the amount of data involved. The latter involve a single measurement point at the cross-section between the grid and the load under consideration. They are less accurate but more easily applied.

Some of the single-point methods that have been proposed involve the construction of a Thevenin or Norton equivalent circuit in order to determine the dominant harmonic source. An important requirement is the accurate estimation of the utility side and customer side equivalent impedances or admittances. A traditional single-point method is based on the determination of the direction of the harmonic active power flow with respect to the fundamental active power at the point of connection of a load. By measuring harmonic voltage and current rms values and phase difference angles at the point of connection, the signs of individual harmonic active powers are derived. A bidirectional active power flow indicates that the load generates harmonics. However, it has been demonstrated that in certain situations a bidirectional flow will not occur even though the load is nonlinear [12]. This approach may also fail to reveal a nonlinear load simply because the values of harmonic active (and reactive) components are very low, as it is often the case in real scenarios. Due to these considerations, more recent methods focus on non-active components of previously defined apparent power equations [8–11]. More specifically, the proposed distorting load identification criteria are based on some kind of distortion power. This distortion power is defined as one of the components of an apparent power equation. A common characteristic of such expressions is the fact that the conservation principle does not apply to them.

In [8], Budeanu's distortion power is used in order to determine whether a load is nonlinear. This power quantity is defined as

$$D_B = \sqrt{S^2 - P^2 - Q_B^2} \tag{1}$$

where S is the apparent power and P is the active power. Also Q_B is defined as

$$Q_B = \sum_i U_i I_i \sin \varphi_i \tag{2}$$

where U_i, I_i are the rms values of the i-th harmonic voltage and current respectively and φ_i their phase difference.

Power quantities defined in IEEE Std. 1459 [13] have also been considered for the identification of distorting loads [9,10]. The apparent power equation suggested by IEEE Std. 1459 is the following.

$$S^2 = (U_1 I_1)^2 + (U_1 I_H)^2 + (U_H I_1)^2 + (U_H I_H)^2 = S_1^2 + D_I^2 + D_V^2 + S_H^2 = S_1^2 + D^2 \tag{3}$$

where $S_I = U_1 I_1$ is the fundamental apparent power, $D_I = U_1 I_H$ is the current distortion power, $D_V = U_H I_1$ is the voltage distortion power and $S_H = U_H I_H$ is the harmonic apparent power. Furthermore, if U, I are the rms values of the voltage and current, then

$$U_H^2 = U^2 - U_1^2 = \sum_{h \neq 1} U_h^2 \tag{4}$$

and

$$I_H^2 = I^2 - I_1^2 = \sum_{h \neq 1} I_h^2 \tag{5}$$

In [11], an approach was presented based on the comparison of three different nonactive powers found in the literature. The three quantities are the fundamental reactive power, i.e.,

$$Q_{11} = U_1 I_1 \sin \varphi_1 \tag{6}$$

Fryze's reactive power, defined as

$$Q_F = \sqrt{S^2 - P^2} \tag{7}$$

and Sharon's quadrature reactive power, defined as

$$S_Q = U \sqrt{\sum_i I_i^2 \sin^2 \varphi_i} \tag{8}$$

The fundamental reactive power Q_{11} is considered as a minimum reference value, since it will usually be nonzero, even in the absence of harmonics. Q_F is the nonactive power written as a single entity and equals Q_{11} in the sinusoidal case. S_Q assumes an intermediate value between Q_{11} and Q_F. If the value of S_Q is closer to Q_{11} than to Q_F, then the source of harmonic pollution is assumed to be upstream from the metering point, otherwise the source of harmonic pollution is assumed to be downstream from the metering point.

1.3. Contribution and paper organization

Distorting load identification based on power components calculated at the load terminals is one of the incentives for the development of a power theory for circuits with periodic, nonsinusoidal waveforms. For decades, the proposed approaches were mainly focused on providing a

decomposition of the apparent power based on various criteria and this is still the norm [13]. However, any apparent power equation can only provide limited information, due to the fact that its terms are squared and often aggregated [14]. This can be an issue even for the sinusoidal case. The apparent power equation $S^2 = P^2 + Q^2$ needs to be accompanied by an expression such as capacitive/inductive for the reactive power. On the other hand, the complex power $\mathbf{S} = P + \mathrm{j}Q$ fully describes power related phenomena at a cross-section between a source and a linear time invariant passive load of any complexity. Its magnitude is equal to the apparent power and its direction and sense are defined by its components on the two axes of the complex plane.

The multidimensionality of voltages and currents under nonsinusoidal conditions does not permit the representation of power by means of complex algebra. Even though current and voltage calculations can be performed using phasor representations for each individual frequency based on the superposition principle, the same principle cannot be applied in power calculations. In [14,15] a novel energy flow model to describe all power components at a cross-section between a source and a load under nonsinusoidal conditions was introduced. An interpretation of the power components in association with an equivalent circuit was presented. For the representation of power, the proposed model was based on the Geometric Algebra (GA) framework [16]. More specifically, a power multivector was introduced, which is fully capable of providing all the necessary information to determine the power components. The apparent power S can be derived as the magnitude of the multivector. The aim of this paper is to investigate the information that can be derived from the components of this power multivector regarding the impact of a load on the distortion at a point of interest.

This paper is organized as follows. The multivectorial representation of power that will be utilized in the proposed approach is briefly outlined in Section 2 and an index for distorting load identification based on this representation is introduced. The determination of the role of a specific load in the distortion at a common point of connection based on this index is presented in Section 3. Simulations using the proposed approach are presented in Section 4. The results are discussed in Section 5. The conclusions are presented in Section 6.

2. Geometric Algebra representation of power

2.1. Formulation of a power multivector

For the following analysis it will be assumed that the voltage and the current contain the same harmonic orders. However, the approach proposed in [14,15] can handle any situation, including the case of harmonics only present in the voltage or the current.

Let us consider the circuit in Figure 1, where a load is supplied by a periodic, nonsinusoidal voltage source. The voltage at the cross-section x-x′ is

$$u(t) = \sqrt{2}U_1 \cos(\omega t + \alpha_1) + \sqrt{2}U_k \cos(k\omega t + \alpha_k) \tag{9}$$

where U_1, U_k are the rms values of the fundamental and the k-th harmonic voltage component respectively and α_1, α_k are the phase angles.

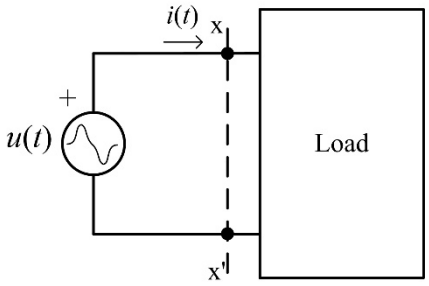

Figure 1. Nonsinusoidal voltage source supplying a load.

The load current will consist of harmonic components of the same order, with rms values I_1, I_k and phase angles β_1, β_k respectively. If $\varphi_i = \alpha_i - \beta_i$, for $i = 1$, k then the current can be decomposed into subcomponents in phase and in quadrature with the corresponding harmonic voltage component, as follows.

$$\begin{aligned} i(t) &= \sqrt{2}I_1\cos(\omega t + \alpha_1 - \varphi_1) + \sqrt{2}I_k\cos(k\omega t + \alpha_k - \varphi_k) \\ &= \sqrt{2}I_1\cos\varphi_1\cos(\omega t + \alpha_1) + \sqrt{2}I_1\sin\varphi_1\sin(\omega t + \alpha_1) \\ &+\sqrt{2}I_k\cos\varphi_k\cos(k\omega t + \alpha_k) + \sqrt{2}I_k\sin\varphi_k\sin(k\omega t + \alpha_k) \end{aligned} \tag{10}$$

Functions $u(t)$ and $i(t)$ are expressed as linear combinations of the four orthonormal basis functions $\left\{\sqrt{2}\cos(\omega t + \alpha_1),\ \sqrt{2}\sin(\omega t + \alpha_1),\ \sqrt{2}\cos(k\omega t + \alpha_k),\ \sqrt{2}\sin(k\omega t + \alpha_k)\right\}$. They can also be represented by vectors **u** and **i** in a 4-dimensional vector space V_4 spanned by 4 orthonormal basis vectors $\{\mathbf{e}_1, \mathbf{e}_2, \mathbf{e}_3, \mathbf{e}_4\}$, which have a one-to-one correspondence with the basis functions, as follows.

$$\mathbf{u} = U_1\mathbf{e}_1 + U_k\mathbf{e}_3 \tag{11}$$

and

$$\mathbf{i} = I_1\cos\varphi_1\mathbf{e}_1 + I_1\sin\varphi_1\mathbf{e}_2 + I_k\cos\varphi_k\mathbf{e}_3 + I_k\sin\varphi_k\mathbf{e}_4 \tag{12}$$

The vectors of V_4 generate a larger linear space, the geometric algebra G_4 of V_4 which is spanned by $\{1, \mathbf{e}_1, \mathbf{e}_2, \mathbf{e}_3, \mathbf{e}_4, \mathbf{e}_{12}, \mathbf{e}_{13}, \mathbf{e}_{14}, \mathbf{e}_{23}, \mathbf{e}_{24}, \mathbf{e}_{34}, \mathbf{e}_{123}, \mathbf{e}_{124}, \mathbf{e}_{134}, \mathbf{e}_{234}, \mathbf{e}_{1234}\}$. In this basis, 1 is a scalar, $\mathbf{e}_1$, $\mathbf{e}_2$, $\mathbf{e}_3$, $\mathbf{e}_4$ are unit vectors, $\mathbf{e}_{12}$, $\mathbf{e}_{13}$, $\mathbf{e}_{14}$, $\mathbf{e}_{23}$, $\mathbf{e}_{24}$, $\mathbf{e}_{34}$ are unit bivectors, $\mathbf{e}_{123}$, $\mathbf{e}_{124}$, $\mathbf{e}_{134}$, $\mathbf{e}_{234}$ are unit 3-vectors and $\mathbf{e}_{1234}$ is a unit 4-vector.

Power can be expressed as a multivector **S** in G_4 generated by the geometric product of the voltage and current vectors, i.e.,

$$\mathbf{S} = \mathbf{ui} \tag{13}$$

The power multivector **S** can be calculated by using (11), (12) and (13), along with the following rules:

1) The geometric product of two basis vectors generates a basis bivector, for example $\mathbf{e}_1\mathbf{e}_2 = \mathbf{e}_{12}$.

2) A basis vector squares to +1, for example $\mathbf{e}_1\mathbf{e}_1 = 1$.

The power multivector **S** at the cross-section x-x′ can be written as follows:

$$\mathbf{S} = \left(P_{11} + Q_{11}\mathbf{e}_{12} + P_{M1k}\mathbf{e}_{13} + Q_{M1k}\mathbf{e}_{14}\right) + \left(P_{kk} + Q_{kk}\mathbf{e}_{34} + P_{Mk1}\mathbf{e}_{31} + Q_{Mk1}\mathbf{e}_{32}\right) \tag{14}$$

where $P_{ii} = U_iI_i\cos\varphi_i$, $Q_{ii} = U_iI_i\sin\varphi_i$, $P_{Mij} = U_iI_j\cos\varphi_j$, $Q_{Mij} = U_iI_j\sin\varphi_j$, $i = 1, k$ and $j = 1, k$.

By grouping together terms of the same nature it can be written that

$$\mathbf{S} = \left(P_{11} + P_{kk}\right) + \left(Q_{11}\mathbf{e}_{12} + Q_{kk}\mathbf{e}_{34}\right) + \left(P_{M1k}\mathbf{e}_{13} + P_{Mk1}\mathbf{e}_{31}\right) + \left(Q_{M1k}\mathbf{e}_{14} + Q_{Mk1}\mathbf{e}_{32}\right) \tag{15}$$

Power is therefore represented by a multivector that consists of a scalar part corresponding to average power and a bivector part corresponding to nonactive power. The bivector part is expressed as a linear combination of basis bivectors. All components are defined through their magnitude, direction and sense. More specifically, there are scalar terms P_{ii} associated with active power in each harmonic. Also, there are bivectorial, nonactive power terms, uselessly contributing to the increase of the apparent power. Bivectorial terms are associated with current components that are either in phase or in quadrature with a voltage component. The symbol P is used to designate the former and the symbol Q is used to designate the latter. Bivectorial terms with magnitude Q_{ii} correspond to the reactive power in each harmonic. The remaining terms with magnitudes of the form P_{Mij} and Q_{Mij} can be associated with a mutual coupling effect attributed to the difference in frequency between the currents $i_1(t)$ and $i_k(t)$ [15]. It should be noted that at the terminals of purely reactive elements P_{Mij} terms are zero. A predominantly capacitive element, such as a compensation capacitor, can thus readily be identified.

It was shown in [14] that the power multivector in its analytic form (14) can successfully demonstrate the bidirectional active power flow that occurs when a nonlinear/time-varying load is supplied by a sinusoidal voltage source with internal impedance. When a bidirectional active power flow is detected, then the presence of a harmonic source in the load side is confirmed. However, as it was demonstrated in [12], when the source voltage is non-sinusoidal, then, in the case of harmonics produced in the load side that are also present in the source voltage, the direction of active power is affected by the relative phase angle between the two harmonic sources. This means that even when harmonic active powers at the metering point turn out to be positive it cannot be safely assumed that there is no harmonic source in the load side. Therefore, in this paper, another part of the power multivector will be utilized in the identification of distorting loads.

By using bold notation to denote individual bivectorial terms, it can be written that

$$\mathbf{S} = \left(P_{11} + P_{kk}\right) + \left(\mathbf{Q}_{11} + \mathbf{Q}_{kk}\right) + \left(\mathbf{P}_{M1k} + \mathbf{P}_{Mk1}\right) + \left(\mathbf{Q}_{M1k} + \mathbf{Q}_{Mk1}\right) \tag{16}$$

or, more concisely,

$$\mathbf{S} = P + \mathbf{Q} + \mathbf{P}_M + \mathbf{Q}_M \tag{17}$$

where

$$P = \sum_i P_{ii} \tag{18}$$

$$\mathbf{Q} = \sum_{i} \mathbf{Q}_{ii} \tag{19}$$

$$\mathbf{P}_M = \sum_{\substack{i,j \\ i \neq j}} \mathbf{P}_{Mij} \tag{20}$$

$$\mathbf{Q}_M = \sum_{\substack{i,j \\ i \neq j}} \mathbf{Q}_{Mij} \tag{21}$$

Furthermore, it can be observed that terms $\mathbf{P}_{M1k} = P_{M1k}\mathbf{e}_{13}$ and $\mathbf{P}_{Mk1} = P_{Mk1}\mathbf{e}_{31}$ have the same direction and opposite sense, due to the fact that $\mathbf{e}_{13} = -\mathbf{e}_{31}$. In the case of $i = 1$, k and $j = 1$, k, the power multivector $\mathbf{S}$ can thus be rewritten in the compact form

$$\mathbf{S} = \left(P_{11} + P_{kk}\right) + \left(P_{M1k} - P_{Mk1}\right)\mathbf{e}_{13} + Q_{11}\mathbf{e}_{12} + Q_{kk}\mathbf{e}_{34} + Q_{M1k}\mathbf{e}_{14} + Q_{Mk1}\mathbf{e}_{32} \tag{22}$$

In a more general situation including multiple harmonics, the terms of $\mathbf{P}_M$ can be grouped into pairs of identical direction but opposite sense, as follows.

$$\mathbf{P}_M = \sum_{\substack{i,j \\ i < j}} \left(\mathbf{P}_{Mij} + \mathbf{P}_{Mji}\right) \tag{23}$$

In [14], it was demonstrated that the total apparent power S is the magnitude of the multivector $\mathbf{S}$. Two apparent power equations can thus be derived. From the analytic form (14) it can be derived that

$$S^2 = \left(P_{11}{}^2 + Q_{11}{}^2 + P_{M1k}{}^2 + Q_{M1k}{}^2\right) + \left(P_{kk}{}^2 + Q_{kk}{}^2 + P_{Mk1}{}^2 + Q_{Mk1}{}^2\right) \tag{24}$$

or, in more general notation,

$$S^2 = \sum_{i} P_{ii}^2 + \sum_{i} Q_{ii}^2 + \sum_{\substack{i,j \\ i \neq j}} P_{Mij}^2 + \sum_{\substack{i,j \\ i \neq j}} Q_{Mij}^2 \tag{25}$$

From the compact form (22) it can be derived that

$$S^2 = \left(P_{11} + P_{kk}\right)^2 + Q_{11}^2 + Q_{kk}^2 + \left(P_{M1k} - P_{Mk1}\right)^2 + Q_{M1k}^2 + Q_{Mk1}^2 \tag{26}$$

or, in more general notation,

$$S^2 = P^2 + Q^2 + P_M^2 + Q_M^2 \tag{27}$$

where

$$P^2 = \left(\sum_i P_{ii} \right)^2 \tag{28}$$

$$Q^2 = \sum_i Q_{ii}^2 \tag{29}$$

$$P_M^2 = \sum_{\substack{i,j \\ i<j}} \left(P_{Mij} - P_{Mji} \right)^2 \tag{30}$$

$$Q_M^2 = \sum_{\substack{i,j \\ i \neq j}} Q_{Mij}^2 \tag{31}$$

2.2. The generalized mutual coupling bivector

It was demonstrated in [14] and [15] that apparent power equations proposed by other methods dealing with power theory can be extracted from (25) or (27). Components of these equations have been utilized in harmonic load identification [8–11]. However, apparent power equations do not include all the necessary information to describe the power components, which may lead to erroneous conclusions.

In (17), the reactive power Q_{11} is not associated with the distortion. Harmonic reactive power components of the form Q_{ii}, $i \neq 1$, are usually relatively small, so they will not be considered either. The remaining bivectorial components will be grouped into a bivector $\mathbf{B}_M$, as follows:

$$\mathbf{B}_M = \mathbf{P}_M + \mathbf{Q}_M = \left(P_{M1k} - P_{Mk1} \right) \mathbf{e}_{13} + Q_{M1k} \mathbf{e}_{14} + Q_{Mk1} \mathbf{e}_{32} \tag{32}$$

Bivector $\mathbf{B}_M$ will be henceforth referred to as the generalized mutual coupling (GMC) bivector due to the nature of the terms it comprises. The formulation of this bivector requires knowledge of the rms values of voltage and current and their phase difference, at every harmonic, at the load terminals.

In a more realistic scenario, with multiple harmonics present, all possible harmonic pairs have to be taken into account in the formulation of bivector $\mathbf{B}_M$. More specifically, if there are H harmonics present in the circuit, including the fundamental, and N possible pairs of harmonics, then for harmonics of orders l and m ($l \neq m$), forming pair z, it can be written that

$$\mathbf{B}_{Mx,z} = \left(P_{Mx,lm} - P_{Mx,ml} \right) \mathbf{e}_{ac} + Q_{Mx,lm} \mathbf{e}_{ad} + Q_{Mx,ml} \mathbf{e}_{cb} \tag{33}$$

where $\mathbf{e}_a$, $\mathbf{e}_b$ and $\mathbf{e}_c$, $\mathbf{e}_d$ are pairs of basis vectors uniquely associated with harmonics l and m respectively, with $a \in \{1,3,5,...,2H-1\}$, $b = a + 1$, $c \in \{1,3,5,...,2H-1\}$, $c \neq a$ and $d = c + 1$. Bivector $\mathbf{B}_M$ can then be calculated as the sum of the N bivectors resulting from the N pairs of harmonics.

Another grouping of bivectorial terms may also be useful, depending on the profile of harmonic pollution. More specifically, bivector $\mathbf{B}_M$ can be decomposed into subcomponents involving

different groups of harmonics. For example, $\mathbf{B}_{Mh}$ may contain terms that only involve harmonics of order lower than 50 and $\mathbf{B}_{Msh}$ may contain terms that involve at least one harmonic of order over 50. Then

$$\mathbf{B}_M = \mathbf{B}_{Mh} + \mathbf{B}_{Msh} \tag{34}$$

Harmonics of orders beyond the 50th are called supraharmonics. They have lately gained the attention of researchers due to the impact of supraharmonic sources on neighbouring loads and the fact that, despite their rising levels, there are no regulations in place for their mitigation [17–19]. Indeed, existing standards regarding harmonic limits consider harmonics up to the 50th (or 40th) order. Equipment manufacturers usually produce devices that comply with imposed limitations, but this is often accompanied by a simultaneous increase of the distortion at harmonic orders well beyond the 50th. As a result, significant supraharmonic content can be detected at the point of connection of PV inverters, EV battery chargers etc. Furthermore, even if the bivector $\mathbf{B}_{Msh}$ at the common point of connection of a distribution line turns out to be low, interactions among individual loads may be significant enough to generate noticeable disturbances. The analysis proposed in this paper can provide valuable insight in this case. On the other hand, if enforcing compliance to existing limits is the only objective, then components beyond the 50th don't have to be taken into account at all, and a single bivector including only harmonics up to the 50th order can be considered.

3. Assessment of a distorting load impact

3.1. GMC bivector at the terminals of a load

In order to find the multivector $\mathbf{S}_x$ of a specific load x, the current at the cross-section between the load and the rest of the network has to be analysed into a component parallel to its respective voltage and a component orthogonal to it. This is also true for the multivector at any point along the network, such as the source terminals. However, in order to correlate the two multivectors, they need to be expressed using the same basis.

The cross-section between the source and the rest of the network will be used as a reference, with a voltage given by (9) and a multivector given by (17). All functions referring to the load will then be expressed using the function basis chosen for the source. This means that every phase angle has to be expressed in terms of the phase angle of the respective harmonic of the reference voltage. Equivalently, all vector and multivector expressions corresponding to load x must be expressed using the corresponding geometric algebra basis.

Let us assume that the voltage $u_x(t)$ of load x is of the form

$$u_x(t) = \sqrt{2}U_{x,1}\cos\left(\omega t + \alpha_{x,1}\right) + \sqrt{2}U_{x,k}\cos\left(k\omega t + \alpha_{x,k}\right) \tag{35}$$

where $U_{x,1}$, $U_{x,k}$ are the rms values of the fundamental and the k-th harmonic voltage component respectively and $\alpha_{x,1}$, $\alpha_{x,k}$ are the phase angles. Let $\theta_{x,i} = \alpha_i - \alpha_{x,i,}$ for $i = 1, k$, then

$$u_x(t) = \sqrt{2}U_{x,1}\cos\left(\omega t + \alpha_1 - \theta_{x,1}\right) + \sqrt{2}U_{x,k}\cos\left(k\omega t + \alpha_k - \theta_{x,k}\right) \tag{36}$$

The load current will consist of two harmonic components with rms values $I_{x,1}$, $I_{x,k}$ and phase angles $\beta_{x,1}$, $\beta_{x,k}$ respectively. If $\varphi_{x,i} = \alpha_{x,i} - \beta_{x,i} = \alpha_i - \theta_{x,i} - \beta_{x,i}$, for $i = 1, k$, then the current can be decomposed into subcomponents in phase and in quadrature with the corresponding harmonic voltage component of (36), as follows.

$$\begin{aligned} i_x(t) &= \sqrt{2}I_{x,1}\cos\left(\omega t + \alpha_1 - \theta_{x,1} - \varphi_{x,1}\right) + \sqrt{2}I_{x,k}\cos\left(k\omega t + \alpha_k - \theta_{x,k} - \varphi_{x,k}\right) \\ &= \sqrt{2}I_{x,1}\cos\varphi_{x,1}\cos\left(\omega t + \alpha_1 - \theta_{x,1}\right) + \sqrt{2}I_{x,1}\sin\varphi_1\sin\left(\omega t + \alpha_1 - \theta_{x,1}\right) \\ &+\sqrt{2}I_{x,k}\cos\varphi_k\cos\left(k\omega t + \alpha_k - \theta_{x,k}\right) + \sqrt{2}I_{x,k}\sin\varphi_k\sin\left(k\omega t + \alpha_k - \theta_{x,k}\right) \end{aligned} \tag{37}$$

Any function of the form

$$\sqrt{2}\cos\left(\omega t + \alpha_1 - y_1\right) = \sqrt{2}\cos y_1\cos\left(\omega t + \alpha_1\right) + \sqrt{2}\sin y_1\sin\left(\omega t + \alpha_1\right) \tag{38}$$

can be represented by a vector that results from a rotation of the vector $\mathbf{e}_1$, which lies on the plain defined by the bivector $\mathbf{e}_{12}$, by an angle y_1. This vector can be written as

$$\mathbf{R}_{y1}^{\dagger}\mathbf{e}_1\mathbf{R}_{y1} = \cos y_1\mathbf{e}_1 + \sin y_1\mathbf{e}_2 \tag{39}$$

where $\mathbf{R}_{y1} = \cos(y_1/2) + \mathbf{e}_{12}\sin(y_1/2)$ represents the rotation and $\mathbf{R}_{y1}^{\dagger}$ its reverse. Similarly, a function of the form $\sqrt{2}\sin(\omega t + a_1 - y_1)$ corresponds to

$$\mathbf{R}_{y1}^{\dagger}\mathbf{e}_2\mathbf{R}_{y1} = \cos y_1\mathbf{e}_2 - \sin y_1\mathbf{e}_1 \tag{40}$$

Such representations can be derived for components of any harmonic order. Voltage and current vectors at the load terminals can thus be expressed as follows.

$$\mathbf{u}_x = U_{x,1}\mathbf{R}_{\theta x,1}^{\dagger}\mathbf{e}_1\mathbf{R}_{\theta x,1} + U_{x,k}\mathbf{R}_{\theta x,k}^{\dagger}\mathbf{e}_3\mathbf{R}_{\theta x,k} \tag{41}$$

and

$$\begin{aligned} \mathbf{i}_x &= I_{x,1}\cos\varphi_{x,1}\mathbf{R}_{\theta x,1}^{\dagger}\mathbf{e}_1\mathbf{R}_{\theta x,1} + I_{x,1}\sin\varphi_{x,1}\mathbf{R}_{\theta x,1}^{\dagger}\mathbf{e}_2\mathbf{R}_{\theta x,1} \\ &+I_{x,k}\cos\varphi_{x,k}\mathbf{R}_{\theta x,k}^{\dagger}\mathbf{e}_3\mathbf{R}_{\theta x,k} + I_{x,k}\sin\varphi_{x,k}\mathbf{R}_{\theta x,k}^{\dagger}\mathbf{e}_4\mathbf{R}_{\theta x,k} \end{aligned} \tag{42}$$

where

$$\begin{aligned} \mathbf{R}_{\theta x,1} &= \cos\frac{\theta_{x,1}}{2} + \mathbf{e}_{12}\sin\frac{\theta_{x,1}}{2}, \quad \mathbf{R}_{\theta x,1}^{\dagger} = \cos\frac{\theta_{x,1}}{2} - \mathbf{e}_{12}\sin\frac{\theta_{x,1}}{2} \\ \mathbf{R}_{\theta x,k} &= \cos\frac{\theta_{x,k}}{2} + \mathbf{e}_{34}\sin\frac{\theta_{x,k}}{2}, \quad \mathbf{R}_{\theta x,k}^{\dagger} = \cos\frac{\theta_{x,k}}{2} - \mathbf{e}_{34}\sin\frac{\theta_{x,k}}{2} \end{aligned} \tag{43}$$

The power multivector at the load terminals can be calculated as the geometric product of (41) and (42), i.e.,

$$\mathbf{S}_x = \mathbf{u}_x \mathbf{i}_x \tag{44}$$

This geometric product will contain the following terms.

$$\mathbf{R}^{\dagger}_{\theta x,1}\mathbf{e}_1\mathbf{R}_{\theta x,1}\mathbf{R}^{\dagger}_{\theta x,1}\mathbf{e}_1\mathbf{R}_{\theta x,1} = 1 \tag{45}$$

$$\mathbf{R}^{\dagger}_{\theta x,k}\mathbf{e}_3\mathbf{R}_{\theta x,k}\mathbf{R}^{\dagger}_{\theta x,k}\mathbf{e}_3\mathbf{R}_{\theta x,k} = 1 \tag{46}$$

$$\mathbf{R}^{\dagger}_{\theta x,1}\mathbf{e}_1\mathbf{R}_{\theta x,1}\mathbf{R}^{\dagger}_{\theta x,1}\mathbf{e}_2\mathbf{R}_{\theta x,1} = \mathbf{R}^{\dagger}_{\theta x,1}\mathbf{e}_1\mathbf{e}_2\mathbf{R}_{\theta x,1} = \mathbf{e}_{12} \tag{47}$$

$$\mathbf{R}^{\dagger}_{\theta x,k}\mathbf{e}_3\mathbf{R}_{\theta x,k}\mathbf{R}^{\dagger}_{\theta x,k}\mathbf{e}_4\mathbf{R}_{\theta x,k} = \mathbf{e}_{34} \tag{48}$$

$$\begin{aligned}\mathbf{R}^{\dagger}_{\theta x,1}\mathbf{e}_1\mathbf{R}_{\theta x,1}\mathbf{R}^{\dagger}_{\theta x,k}\mathbf{e}_3\mathbf{R}_{\theta x,k} &= \mathbf{e}_1\left(\cos\theta_{x,1} + \sin\theta_{x,1}\mathbf{e}_{12}\right)\mathbf{e}_3\left(\cos\theta_{x,k} + \sin\theta_{x,k}\mathbf{e}_{34}\right)\\ &= \mathbf{e}_{13}\left(\cos\theta_{x,1} + \sin\theta_{x,1}\mathbf{e}_{12}\right)\left(\cos\theta_{x,k} + \sin\theta_{x,k}\mathbf{e}_{34}\right)\\ &= \mathbf{e}_{13}\mathbf{R}_x\end{aligned} \tag{49}$$

where

$$\mathbf{R}_x = \cos\theta_{x,1}\cos\theta_{x,k} + \cos\theta_{x,1}\sin\theta_{x,k}\mathbf{e}_{34} + \sin\theta_{x,1}\cos\theta_{x,k}\mathbf{e}_{12} + \sin\theta_{x,1}\sin\theta_{x,k}\mathbf{e}_{1234} \tag{50}$$

Similarly

$$\mathbf{R}^{\dagger}_{\theta x,k}\mathbf{e}_3\mathbf{R}_{\theta x,k}\mathbf{R}^{\dagger}_{\theta x,1}\mathbf{e}_1\mathbf{R}_{\theta x,1} = \mathbf{e}_{31}\mathbf{R}_x \tag{51}$$

$$\mathbf{R}^{\dagger}_{\theta x,1}\mathbf{e}_1\mathbf{R}_{\theta x,1}\mathbf{R}^{\dagger}_{\theta x,k}\mathbf{e}_4\mathbf{R}_{\theta x,k} = \mathbf{e}_{14}\mathbf{R}_x \tag{52}$$

$$\mathbf{R}^{\dagger}_{\theta x,k}\mathbf{e}_3\mathbf{R}_{\theta x,k}\mathbf{R}^{\dagger}_{\theta x,1}\mathbf{e}_2\mathbf{R}_{\theta x,1} = \mathbf{e}_{32}\mathbf{R}_x \tag{53}$$

due to $\mathbf{e}_{3412} = \mathbf{e}_{1234}$.

Therefore, the power multivector of the load in the new basis can be written as

$$\mathbf{S}_x = P_{x,11} + P_{x,kk} + Q_{x,11}\mathbf{e}_{12} + Q_{x,kk}\mathbf{e}_{34} + \left(P_{Mx,1k} - P_{Mx,k1}\right)\mathbf{e}_{13}\mathbf{R}_x + Q_{Mx,1k}\mathbf{e}_{14}\mathbf{R}_x + Q_{Mx,k1}\mathbf{e}_{32}\mathbf{R}_x \tag{54}$$

where $P_{x,ii} = U_{x,i}I_{x,i}\cos\varphi_{x,i}$, $Q_{x,ii} = U_{x,i}I_{x,i}\sin\varphi_{x,i}$, $P_{Mx,ij} = U_{x,i}I_{x,j}\cos\varphi_{x,j}$, $Q_{Mx,ij} = U_{x,i}I_{x,j}\sin\varphi_{x,j}$, $i = 1, k$ and $j = 1, k$.

It can thus be deduced that active and reactive power components of the form $P_{x,ii}$ and $Q_{x,ii}$ are not affected by the basis change. The remaining terms are grouped into the GMC bivector of the load $\mathbf{B}_{Mx}$. The magnitude of this bivector is preserved in the new basis, but individual subcomponents are transformed as follows.

$$\mathbf{B}_{Mx} = \left[\left(P_{Mx,1k} - P_{Mx,k1} \right) \mathbf{e}_{13} + Q_{Mx,1k} \mathbf{e}_{14} + Q_{Mx,k1} \mathbf{e}_{32} \right] \mathbf{R}_x \tag{55}$$

The multivector $\mathbf{R}_x$ is associated with the phase angle difference between the voltage at the reference terminals and the voltage at the terminals of load *x*. When there are multiple harmonics present, then more of these multivectors have to be derived, one for each possible harmonics pair. More specifically, for harmonics of orders *l* and *m* ($l \neq m$), forming pair *z*, it can be written that

$$\mathbf{B}_{Mx,z} = \left[\left(P_{Mx,lm} - P_{Mx,ml} \right) \mathbf{e}_{ac} + Q_{Mx,lm} \mathbf{e}_{ad} + Q_{Mx,ml} \mathbf{e}_{cb} \right] \mathbf{R}_{x,z} \tag{56}$$

where

$$\mathbf{R}_{x,z} = \cos\theta_{x,l} \cos\theta_{x,m} + \cos\theta_{x,l} \sin\theta_{x,m} \mathbf{e}_{cd} + \sin\theta_{x,l} \cos\theta_{x,m} \mathbf{e}_{ab} + \sin\theta_{x,l} \sin\theta_{x,m} \mathbf{e}_{abcd} \tag{57}$$

Then the GMC bivector of element *x* can be calculated as the sum of the *N* bivectors resulting from the *N* pairs of harmonics. It should be noted here that a different approach is possible. All voltage and current functions could have been expressed in terms of the orthonormal basis functions $\{\sqrt{2}\cos\omega t,\ \sqrt{2}\sin\omega t,\ \sqrt{2}\cos k\omega t,\ \sqrt{2}\sin k\omega t\}$. Components P_{ii}, Q_{ii} would not be affected, but the remaining bivectorial components would have no distinguishing characteristic. This could be counterintuitive when mitigation of such components with passive elements is an objective.

3.2. Conservation of power multivector components

According to Tellegen's theorem the sum of the power of all circuit components is zero, or, equivalently, the power delivered to the network is equal to the power that is received. Every power quantity that results as a product of quantities that represent voltage and current and are subject to KVL and KCL constraints complies with this theorem. Voltage and current vectors are such quantities, and thus the power multivector **S** is conservative.

For a network with various loads the multivector **S** at the cross-section between the source and the rest of the network can be written as

$$\mathbf{S} = \sum_n \mathbf{S}_n \tag{58}$$

where $\mathbf{S}_n$ is the power multivector of load *n.* This subscript will be used to denote all quantities referring to this load.

The scalar parts of the power multivectors represent active power components and their sum equals the active power of the source. More specifically, from (22) and (54) it can be deduced that

$$P_{11} + P_{kk} = \sum_n \left(P_{n,11} + P_{n,kk} \right) \tag{59}$$

Reactive power bivectors of the form $\mathbf{Q}_{ii}$ are independent from the rest of the multivector terms, as indicated by their respective basis bivectors in (22) and (54). Therefore, for every harmonic order, the sum of the reactive power bivectors of the loads equals the reactive power bivector of the source. More specifically, for the fundamental frequency it is

$$Q_{11}\mathbf{e}_{12} = \sum_n Q_{n,11}\mathbf{e}_{12} \tag{60}$$

and for the *k*-th harmonic order it is

$$Q_{kk}\mathbf{e}_{34} = \sum_n Q_{n,kk}\mathbf{e}_{34} \tag{61}$$

The remaining power multivector components constitute $\mathbf{B}_M$. From (22), (54), (59)–(61), it can be deduced that

$$\mathbf{B}_M = \sum_n \mathbf{B}_{Mn} \tag{62}$$

This equation is valid at the cross-section between the source and the rest of the network, regardless of the way the loads are connected. By associating $\mathbf{B}_{Mx}$ with $\mathbf{B}_M$ the impact of load *x* on $\mathbf{B}_M$ can be assessed.

3.3. Contribution of a load to the GMC bivector at the supply terminals

According to (62), the GMC bivector at the supply terminals equals the sum of the GMC bivectors of the loads. Each of the load bivectors in (62) has its own magnitude, direction and sense. They counteract each other in every other direction but the direction of $\mathbf{B}_M$. Each of them can thus be decomposed into a component parallel to $\mathbf{B}_M$ and a component orthogonal to it.

If bivector $\mathbf{B}_{Mx}$ of load *x* is decomposed into a parallel component $\mathbf{B}_{Mxp}$ and an orthogonal component $\mathbf{B}_{Mxr}$, then the former will represent the part of $\mathbf{B}_{Mx}$ that participates in $\mathbf{B}_M$ and the latter the remaining part of $\mathbf{B}_{Mx}$. The sum of the parallel components of all load bivectors equals $\mathbf{B}_M$, whereas the sum of the orthogonal components equals zero. The parallel component can be associated with an energy exchange between the load and the source, whereas the orthogonal component with energy interactions of the loads, as perceived by the source.

The parallel component $\mathbf{B}_{Mxp}$ can be expressed as

$$\mathbf{B}_{Mxp} = b_{Mx}\mathbf{B}_M \tag{63}$$

where b_{Mx} is a signed scalar coefficient. Component $\mathbf{B}_{Mxp}$ has the same direction as $\mathbf{B}_M$ and magnitude and sense given by $b_{Mx}B_M$, where B_M is the magnitude of $\mathbf{B}_M$. It can be calculated as a projection in GA, i.e.,

$$\mathbf{B}_{Mxp} = \left(\mathbf{B}_{Mx} \cdot \mathbf{B}_M\right)\mathbf{B}_M^{-1} \tag{64}$$

where $\mathbf{B}_M^{-1}$ is the inverse of $\mathbf{B}_M$ and $\mathbf{B}_{Mx} \cdot \mathbf{B}_M$ the inner product of the two bivectors. Furthermore,

$$\mathbf{B}_M^{-1} = \frac{\mathbf{B}_M^{\dagger}}{B_M^2} \tag{65}$$

where $\mathbf{B}_M^\dagger$ is the reverse of $\mathbf{B}_M$. Due to the fact that $\mathbf{B}_M$ is a bivector, the inner product can be calculated as the scalar part $\langle \mathbf{B}_{Mx}\mathbf{B}_M \rangle_0$ of the geometric product $\mathbf{B}_{Mx}\mathbf{B}_M$. Furthermore, the reverse can be calculated as follows.

$$\mathbf{B}_M^\dagger = -\mathbf{B}_M \tag{66}$$

Therefore,

$$\mathbf{B}_{Mxp} = \langle \mathbf{B}_{Mx}\mathbf{B}_M \rangle_0 \frac{\mathbf{B}_M^\dagger}{B_M^2} = \frac{\langle \mathbf{B}_{Mx}\mathbf{B}_M^\dagger \rangle_0}{B_M^2}\mathbf{B}_M \tag{67}$$

Coefficient b_{Mx} can thus be calculated as follows:

$$b_{Mx} = \frac{\langle \mathbf{B}_{Mx}\mathbf{B}_M^\dagger \rangle_0}{B_M^2} \tag{68}$$

When all the loads are taken into account, then

$$\sum_n b_{Mn} = \sum_n \frac{\langle \mathbf{B}_{Mn}\mathbf{B}_M^\dagger \rangle_0}{B_M^2} = \frac{\langle \mathbf{B}_M\mathbf{B}_M^\dagger \rangle_0}{B_M^2} = 1 \tag{69}$$

Furthermore, if supraharmonics and lower order harmonics are examined separately and $\mathbf{B}_M$ is decomposed into $\mathbf{B}_{Mh}$ and $\mathbf{B}_{Msh}$, then two distinct coefficients can be derived, i.e., b_{Mhx} and b_{Mshx}.

4. Examples

Let us consider the circuit in Figure 2, where a nonideal source is supplying two loads, one of which is nonlinear.

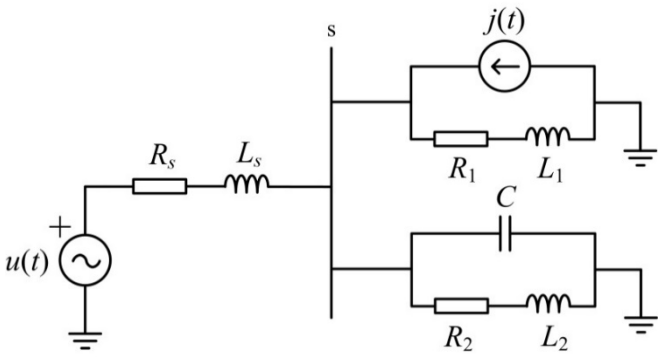

Figure 2. Sinusoidal source with internal impedance supplying a linear and a nonlinear load.

For the source: R_S = 0.01 Ω, L_S = 2 mH, for the loads: R_1 = 9 Ω, L_1 = 12 mH, R_2 = 7 Ω, L_2 = 30 mH. The capacitor has C = 125 μF and is considered separately. Furthermore,

$$u(t) = 230\sqrt{2}\cos\omega t \ \ \text{(V)} \tag{70}$$

$$j(t) = 2\sqrt{2}\cos 17\omega t \ \ \text{(A)} \tag{71}$$

The GMC bivectors of the circuit components are

$$\mathbf{B}_{M1} = -75.3\mathbf{e}_{13} + 450.9\mathbf{e}_{14} + 31.5\mathbf{e}_{32} \ \ \text{(VA)} \tag{72}$$

$$\mathbf{B}_{M2} = -40.1\mathbf{e}_{13} + 4.9\mathbf{e}_{14} + 54.3\mathbf{e}_{32} \ \ \text{(VA)} \tag{73}$$

$$\mathbf{B}_{MC} = -530.1\mathbf{e}_{14} - 31.2\mathbf{e}_{32} \ \ \text{(VA)} \tag{74}$$

The GMC bivector at point s, which is considered to be the common point of connection of all loads, is

$$\mathbf{B}_{M} = -115.4\mathbf{e}_{13} - 74.3\mathbf{e}_{14} + 54.6\mathbf{e}_{32} \ \ \text{(VA)} \tag{75}$$

A summation of individual circuit element bivectors results in $\mathbf{B}_M$, as expected. However, from the viewpoint of s, the loads are responsible for the following:

$$\mathbf{B}_{M1p} = 122.2\mathbf{e}_{13} + 78.7\mathbf{e}_{14} - 57.7\mathbf{e}_{32} \ \ \text{(VA)} \tag{76}$$

$$\mathbf{B}_{M2p} = -38.2\mathbf{e}_{13} - 24.6\mathbf{e}_{14} + 18.1\mathbf{e}_{32} \ \ \text{(VA)} \tag{77}$$

$$\mathbf{B}_{MCp} = -199.4\mathbf{e}_{13} - 128.4\mathbf{e}_{14} + 94.2\mathbf{e}_{32} \ \ \text{(VA)} \tag{78}$$

The remaining components, indicating load interactions, are

$$\mathbf{B}_{M1r} = \mathbf{B}_{M1} - \mathbf{B}_{M1p} = -197.5\mathbf{e}_{13} + 372.2\mathbf{e}_{14} + 89.2\mathbf{e}_{32} \ \ \text{(VA)} \tag{79}$$

$$\mathbf{B}_{M2r} = \mathbf{B}_{M2} - \mathbf{B}_{M2p} = -1.9\mathbf{e}_{13} + 29.5\mathbf{e}_{14} + 36.2\mathbf{e}_{32} \ \ \text{(VA)} \tag{80}$$

$$\mathbf{B}_{MCr} = \mathbf{B}_{MC} - \mathbf{B}_{MCp} = 199.4\mathbf{e}_{13} - 401.7\mathbf{e}_{14} - 125.4\mathbf{e}_{32} \ \ \text{(VA)} \tag{81}$$

The magnitudes of the bivectors of the loads are B_{M1} = 458.2 VA, B_{M2} = 67.7 VA, B_{MC} = 531.0 VA. At first glance, the capacitor behaviour seems to be similar to that of the nonlinear load, or even more disruptive. However, the bivector components of the capacitor happen to counteract the respective components of the nonlinear load, i.e., when one circuit element delivers power the other receives. This observation would not be possible just by inspecting bivector magnitudes, or any index based on apparent power components. For example, the harmonic apparent power S_H

according to IEEE Std. 1459 [13] is 0.1 VA for the linear load, 7.4 VA for the nonlinear load and 8.8 VA for the capacitor.

Let us consider the circuit in Figure 3, where a nonideal source is supplying three loads, two of which are nonlinear.

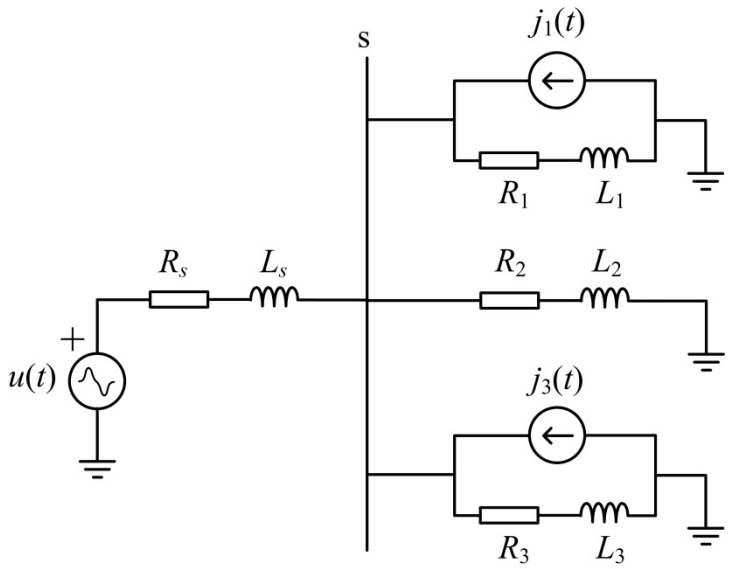

Figure 3. Sinusoidal source with internal impedance supplying a linear and two nonlinear loads.

For the source: R_S = 0.01 Ω, L_S = 2 mH, for the loads: $R_1 = R_3$ = 9 Ω, $L_1 = L_3$ = 12 mH, R_2 = 7 Ω, L_2 = 30 mH. Furthermore,

$$u(t) = 230\sqrt{2}\cos\omega t + 10\sqrt{2}\cos 5\omega t \quad \text{(V)} \tag{82}$$

$$j_1(t) = 5\sqrt{2}\cos 5\omega t \quad \text{(A)} \tag{83}$$

$$j_3(t) = 5\sqrt{2}\cos\left(5\omega t + \gamma\right) \quad \text{(A)} \tag{84}$$

Various indices that have been proposed for load identification have been calculated and are presented in Table 1 for $\gamma = 0^o$ and in Table 2 for $\gamma = 180^o$. The GMC bivector magnitudes and b_M coefficients have also been included.

In the case of Table 1, the Total Harmonic Distortion indices for the current and the voltage at the common point of connection s are *ITHD* = 12.2% and *VTHD* = 11.8% respectively. The two identical nonlinear loads equally contribute to the GMC bivector magnitude at point s. More specifically, they are each responsible for 0.451·2404.7 = 1084.5 VA of the total 2404.7 VA at point s.

In the case of Table 2 the distortion at the supply terminals is radically reduced. More specifically, *ITHD* = 1.5% and *VTHD* = 3.6%. This is evident in the GMC bivector magnitude, as well as the rest of the indices calculated at point s. However, the participation of each harmonic source has to be determined. According to the harmonic apparent power S_H defined in IEEE Std. 1459 the two sources seem almost equally disruptive. The triplet of Q_{11}, S_Q and Q_F does not differentiate

the two loads either. According to Budeanu's distortion power D_B and the GMC bivector magnitude the two sources are somewhat differentiated, but important information is still missing. It should also be noted that there is no bidirectional active power flow at the point of connection of load 3. More specifically, the fundamental active power is 4093.5 W, the 5th harmonic active power is 38.1 W and they both have positive signs. Therefore, the harmonic active power flow direction does not provide helpful information. On the other hand, by examining the b_M coefficients for the two loads it can be deduced that load 1 contributes 2.281·413.9 = 944.1 VA, whereas load 3 mitigates the disturbance by 1.583·413.9 = 655.2 VA, as indicated by the sign of its b_M coefficient.

Table 1. Various indices for the loads of Figure 3 when $\gamma = 0^o$.

Circuit terminals	S_H (VA)	D (VA)	D_B (VA)	Q_{11} (Var)	S_Q (VA)	Q_F (VA)	B_M (VA)	b_M
Load 1	93.9	957.4	1227.4	1714.7	1877.3	2039.1	1100.2	0.451
Load 2	12.7	448.3	344.3	2961.3	2983.7	2993.7	438.9	0.098
Load 3	93.9	957.4	1227.4	1714.7	1877.3	2039.1	1100.2	0.451
Point s	175.6	2077.7	2798.1	6390.6	6578.6	6830.0	2404.7	1

Table 2. Various indices for the loads of Figure 3 when $\gamma = 180^o$.

Circuit terminals	S_H (VA)	D (VA)	D_B (VA)	Q_{11} (Var)	S_Q (VA)	Q_F (VA)	B_M (VA)	b_M
Load 1	36.4	1030.9	1154.9	1714.7	1724.6	2072.5	1164.1	2.281
Load 2	1.2	135.8	104.3	2961.3	2963.4	2964.3	133.0	0.303
Load 3	38.2	1080.0	926.2	1714.7	1716.2	1947.5	923.5	−1.583
Point s	6.4	471.5	309.0	6390.6	6396.9	6404.0	413.9	1

Let us now consider the circuit in Figure 4.

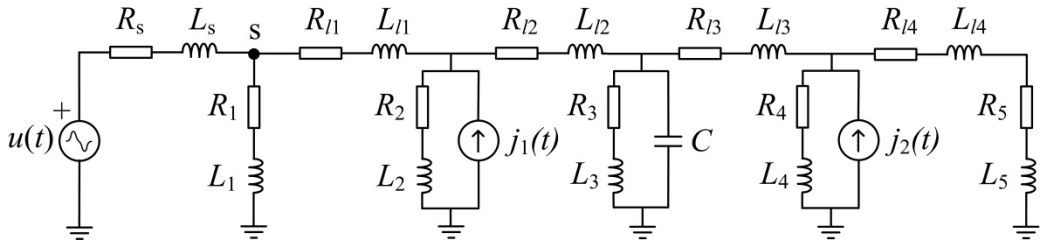

Figure 4. Nonsinusoidal source supplying a combination of linear and nonlinear loads.

For the source: $R_S = 0.0002$ Ω, $L_S = 0.06$ mH, for the loads: $R_1 = 14$ Ω, $L_1 = 16$ mH, $R_2 = 12$ Ω, $L_2 = 20$ mH, $R_3 = 8$ Ω, $L_3 = 25$ mH, $R_4 = 15$ Ω, $L_4 = 15$ mH, $R_5 = 10$ Ω, $L_5 = 14$ mH, for the connecting line segments: $R_{l1} = 0.005$ Ω, $L_{l1} = 0.05$ mH, $R_{l2} = 0.01$ Ω, $L_{l2} = 0.1$ mH, $R_{l3} = 0.02$ Ω, $L_{l3} = 0.2$ mH, $R_{l4} = 0.01$ Ω, $L_{l4} = 0.1$ mH. The capacitor has $C = 120$ μF and is considered separately. Furthermore,

$$u(t) = 230\sqrt{2}\cos\omega t + 20\sqrt{2}\cos 5\omega t + 10\sqrt{2}\cos 7\omega t \quad \text{(V)} \tag{85}$$

$$j_1(t) = 10\sqrt{2}\cos(5\omega t + 210°) + 7\sqrt{2}\cos(7\omega t + 250°) + 0.4\sqrt{2}\cos 100\omega t \quad \text{(A)} \tag{86}$$

$$j_2(t) = 12\sqrt{2}\cos(5\omega t + 190°) + 8\sqrt{2}\cos(7\omega t + 50°) + 0.8\sqrt{2}\cos 100\omega t \quad \text{(A)} \tag{87}$$

In this case, a one-by-one comparison of bivector terms is neither practical nor helpful. B_{Mh}, B_{Msh} of all loads and b_{Mh}, b_{Msh} coefficients are shown in Table 3.

Table 3. GMC bivector magnitudes and b_M coefficients of all circuit components for harmonic and supraharmonic content.

Circuit terminals	B_{Mh} (VA)	b_{Mh}	B_{Msh} (VA)	b_{Msh}
Load 1	322.4	−0.044	4.3	0.054
Load 2	2506.0	0.440	92.4	1.932
Load 3	498.5	−0.043	5.6	−0.066
Load 4	3111.8	0.557	203.2	4.602
Load 5	477.7	−0.068	95.0	1.206
Capacitor	1154.6	0.157	235.9	−4.611
Line 1	128.9	−0.002	16.7	−0.228
Line 2	134.5	0.002	41.5	0.562
Line 3	190.0	0.000	185.4	−2.459
Line 4	3.4	−0.000	0.7	0.009
Point s	4297.1	1	41.8	1

Table 3 indicates that the GMC bivector at point s is mainly affected by loads 2 and 4, as well as the capacitor. However, as indicated by b_{Mhx}, the actual impact of the capacitor on the bivector at point s is less critical. Furthermore, by examining the distortion associated with the supraharmonic (h = 100) in the current, it can be deduced that the capacitor has a mitigating effect. This could be detrimental to the capacitor, but that is beyond the scope of this paper. It should be noted that, in this case, there is no bidirectional active power flow at the point of connection of load 2, so the harmonic active power flow direction does not provide helpful information.

5. Discussion

In the examples of Section 4, the GMC bivector was used in order to assess the impact of a load on the distortion at a common point of connection. Its unique feature is the fact that it contains information regarding not only magnitude, but also direction and sense. The magnitude can serve as an indicator of a distorting load just like other indices proposed by methods based on components of an apparent power equation, but the additional information included in the bivector can also reveal whether the load adds to the overall distortion or acts in a mitigating manner. Furthermore, its conservative nature permits an association between the distortion at the load terminals and a common point of connection where the distortion has to be assessed and regulated. This particular feature is missing from the apparent power, as well as any components derived from possible decompositions of that quantity.

According to the proposed approach all loads can be viewed as black boxes. As long as the voltage and current phasors at every harmonic are available at the load terminals, either through measurements or calculations, then the proposed bivector can be derived. However, a common

concern with single-point methods is the fact that load current harmonics flowing through the supply system impedance cause a corresponding voltage drop that affects the voltage supply of every load in the circuit. As a result, nonlinear loads contribute to the harmonic pollution in the supply voltage, interfering with the harmonic current emissions of other loads and even causing harmonic emissions from linear loads. A severely distorted voltage can cause large linear loads to produce unexpectedly high harmonic currents. In such cases, linear loads can be mistaken for nonlinear ones, even though they are not to blame for the distortion. On the other hand, a moderate voltage distortion will also result in harmonic current injection from linear loads, but the associated B_M magnitude will be low. Therefore, the presented approach is based on the assumption that voltage distortion is moderate. This assumption is common among single-point methods and is based on the observation that the control of the supply voltage harmonics is the responsibility of the utility and that normally the necessary measures to ensure compliance with standard limits will be taken.

In the examples presented in Section 4 the circuits are assumed to be supplied by voltage sources with nonzero impedance. In addition, a distorted source voltage waveform was considered in the second circuit. The harmonic distortion of the load voltages is considerable. Due to this fact, the linear loads participate in the distortion at point s. However, their contribution is not comparable to that of nonlinear loads. On the other hand, in the circuit of Figure 4 the contribution of load 5 to the supraharmonic distortion at point s ended up being unexpectedly high, even though no supraharmonic was included in the source voltage. This is due to the supraharmonic currents injected by the nonlinear loads, which, at first glance, could be considered insignificant. However, these currents combined with the high impedance of the line in this frequency resulted in a considerable supraharmonic component in the voltage supply of the loads. The necessity for regulations dealing with consumers generating supraharmonics is evident.

In the examples of Figure 2 and Figure 4 of Section 4 capacitors are included in the circuits. Depending on the order of the harmonics present in the system, capacitors appear to either enhance or mitigate the distortion. If the former is true, then the presence of the capacitor is causing a disturbance that needs to be addressed. Nevertheless, the impact of a capacitor should be differentiated from that of a nonlinear load. This information is inherent in the bivector, since bivector component $\mathbf{P}_M$ results from components of the form P_{Mij}, which are all zero at the terminals of a capacitor. Therefore, a capacitor cannot be mistaken for a nonlinear load, even if its $\mathbf{B}_M$ bivector magnitude turns out to be comparable to that of a nonlinear load.

However, it should be noted that if the capacitor is considered to be part of a larger installation viewed as a black box and available measurements are strictly limited to the installation terminals, then the overall impact of this installation as a single entity can only be assessed. The proposed method cannot offer information regarding the exact nature of individual devices inside the black box and their interconnections. If the installation turns out to be exacerbating harmonic distortion, then the necessity for corrective measures will have to be examined. A more detailed study of the installation and its specific components utilizing optimization techniques can reveal the most effective measures for reducing the impact of this installation on harmonic distortion.

6. Conclusions

In this paper, components of a previously introduced power multivector were utilized in the identification of distorting loads. These components were grouped into a single quantity, the

generalized mutual coupling (GMC) bivector $\mathbf{B}_M$, with magnitude, direction and sense. In situations where the magnitude provides ambiguous information, an inspection of its other two attributes can provide useful guidance. When the distortion at a specific point of a network comprising various loads is examined, then the impact of individual loads can be evaluated by means of b_M coefficients. These coefficients assign a part of the GMC bivector at the point of interest to each load. The remaining part of each load bivector is associated with load interactions and has no bearing on the bivector at the point of interest.

Conflict of interest

All authors declare no conflicts of interest in this paper.

References

1. Das SR, Mishra DP, Ray PK, et al. (2021) Power quality improvement using fuzzy logic-based compensation in a hybrid power system, *Int J Power Electron Drive Syst* 12: 576–584. https://doi.org/10.11591/ijpeds.v12.i1.pp576-584
2. Das SR, Mishra AK, Ray PK, et al. (2022) Application of artificial intelligent techniques for power quality improvement in hybrid microgrid system. *Electronics* 11: 3826: 1–19. https://doi.org/10.3390/electronics11223826
3. Das B, Panigrahi PK, Das SR, et al. (2021) Power quality improvement in a photovoltaic based microgrid integrated network using multilevel inverter. *Int J Emerg Electr Power Syst* 23: 197–209. https://doi.org/10.1515/ijeeps-2021-0040
4. Sinvula R, Abo-Al-Ez KM, Kahn MT (2019) Harmonic source detection methods: A systematic literature review. *IEEE Access* 7: 74283–74299. https://doi.org/10.1109/ACCESS.2019.2921149
5. Saxena D, Bhaumik S, Singh SN (2014) Identification of multiple harmonic sources in power system using optimally placed voltage measurement devices. *IEEE Trans Ind Electron* 61: 2483–2492. https://doi.org/10.1109/TIE.2013.2270218
6. Carta D, Muscas C, Pegoraro PA, et al. (2019) Identification and estimation of harmonic sources based on compressive sensing. *IEEE Trans Instrum Meas* 68: 95–104. https://doi.org/10.1109/TIM.2018.2838738
7. Li C, Xu W, Tayjasanant T (2004) A "critical impedance"—based method for identifying harmonic sources. *IEEE Trans Power Deliv* 19: 671–678. https://doi.org/10.1109/TPWRD.2004.825302
8. Stevanović D, Petković P (2015) A single-point method for identification sources of harmonic pollution applicable to standard power meters. *Electr Eng* 97: 165–174. https://doi.org/10.1007/s00202-014-0324-z
9. Li C-S, Bai Z-X, Xiao X-Y, et al. (2016) Research of harmonic distortion power for harmonic source detection. *International Conference on Harmonics and Quality of Power*. IEEE, Belo Horizonte, Brazil, 1–4. https://doi.org/10.1109/ICHQP.2016.7783437

10. Anu G, Fernandez FM (2020) Identification of harmonic injection and distortion power at customer location. *19th International Conference on Harmonics and Quality of Power (ICHQP)*, Dubai, United Arab Emirates, 1–5. https://doi.org/10.1109/ICHQP46026.2020.9177869
11. Cataliotti A, Cosentino V, Nuccio S (2008) Comparison of nonactive powers for the detection of dominant harmonic sources in power systems. *IEEE Trans Instrum Meas* 57: 1554–1561. https://doi.org/10.1109/TIM.2008.925338
12. Xu W, Liu X, Liu Y (2003) An investigation on the validity of power direction method for harmonic source determination. *IEEE Trans Power Deliv* 18: 214–219. https://doi.org/10.1109/TPWRD.2002.803842
13. IEEE Std 1459-2010: IEEE Standard definitions for the measurement of electric power quantities under sinusoidal, nonsinusoidal, balanced, or unbalanced conditions, 2010.
14. Menti A, Zacharias T, Milias-Argitis J (2007) Geometric algebra: a powerful tool for representing power under nonsinusoidal conditions. *IEEE Trans Circuits Syst I, Fundam Theory Appl* 54: 601–609. https://doi.org/10.1109/TCSI.2006.887608
15. Menti A, Zacharias Th, Milias-Argitis J (2010) Power components under nonsinusoidal conditions using a power multivector. *Proc 10th Conference-Seminar International School on Nonsinusoidal Currents and Compensation (ISNCC)*. Lagow, Poland, 174–179. https://doi.org/10.1109/ISNCC.2010.5524495
16. Doran C, Lasenby A (2003) *Geometric Algebra for Physicists*. Cambridge University Press. https://doi.org/10.1017/CBO9780511807497
17. Bollen M, Olofsson M, Larsson A, et al. (2014) Standards for supraharmonics (2 to 150 kHz). *IEEE Electromag Compatibil Mag* 3: 114–119. https://doi.org/10.1109/MEMC.2014.6798813
18. Barkas D, Ioannidis G, Kaminaris S, et al. (2022) Design of a supraharmonic monitoring system based on an FPGA device. *Sensors* 22: 1–20. https://doi.org/10.3390/s22052027
19. Menti A, Barkas D, Kaminaris S, et al. (2012) Supraharmonic emission from a three-phase PV system connected to the LV grid. *Energy Rep* 7: 527–542. https://doi.org/10.1016/j.egyr.2021.07.100

AIMS Press